Supporting Information

15.8% Efficiency All-Small-Molecule Solar Cells Enabled by a Combination of Side-chain Engineering and Polymer Additive

Haiyan Liang,[a] Yang Wang,[a] Xia Guo,*[a] Ding Yang,[a] Xinxin Xia,[b] Jianqiu Wang,[a] Liu Zhang,[a] Yu Shi,[a] Xinhui Lu[b] and Maojie Zhang*[a]

[a]Laboratory of Advanced Optoelectronic Materials, Suzhou Key Laboratory of Novel Semiconductor-optoelectronics Materials and Devices, College of Chemistry, Chemical Engineering and Materials Science, Soochow University, Suzhou 215123, China

E-mail: guoxia@suda.edu.cn; mjzhang@suda.edu.cn

[b]Department of Physics, Chinese University of Hong Kong, New Territories, Hong Kong 999077, P. R. China

Experimental Section

Instruments and Measurements

^{1}H NMR, ^{13}C NMR, TGA, and DSC measurement

^{1}H NMR and ^{13}C NMR spectra were measured in $CDCl_3$ on Bruker AV 400 MHz FT-NMR spectrometer. Thermogravimetric analysis (TGA) was performed on a Perkin-Elmer TGA-7. Differential scanning calorimetry (DSC) was performed on a TA DSC Q-200.

UV-Vis absorption, CV, and PL measurement

UV-vis absorption spectra were taken on an Agilent Technologies Cary Series UV-Vis-

NIR Spectrophotometer. The electrochemical cyclic voltammetry (CV) was performed on a Zahner Ennium IM6 Electrochemical Workstation with glassy carbon disk, Pt wire, and Ag/Ag^+ electrode as working electrode, counter electrode, and reference electrode respectively, in a 0.1 M tetrabutylammonium hexafluorophosphate (Bu4NPF6) acetonitrile solution at a scan rate of 50 mV s^{-1}. Photoluminescence (PL) spectra were performed on an Edinburgh Instrument FLS 980.

***J-V* and EQE measurement**

The current density-voltage (*J-V*) characteristics of the non-fullerene SM-OSCs were recorded with a keithley 2450. The power conversion efficiencies of the SM-OSCs were measured under 1 sun, AM 1.5G (air mass 1.5 global) (100 mW cm^{-2}) using a SS-F5-3A (Enli Technology CO., Ltd.) solar simulator (AAA grade, 50 mm x 50 mm photo-beam size). 2×2 cm^2 Monocrystalline silicon reference cell (SRC-00019, covered with a KG5 filter windows) was purchased from Enli Technology CO., Ltd. The EQE was measured by Solar Cell Spectral Response Measurement System QE-R3011 (Enli Technology CO., Ltd.). The light intensity at each wavelength was calibrated with a standard single-crystal Si photovoltaic cell.

Mobility measurement

The hole and electron mobilities of devices were evaluated from space-charge-limited current (SCLC) method with hole-only structure of ITO/PEDOT:PSS/blend films/MoO_3/Al and electron-only structure of ITO/ZnO/blend films/PDINO/Al, respectively. The corresponding charge mobilities were calculated from fitting the Mott-Gurney square law $J = 9\varepsilon_r\varepsilon_0\mu V^2/(8L^3)$, where J is the current density, ε_r is the

dielectric permittivity of the active layer, ε_0 is the vacuum permittivity, L is the thickness of the active layer, μ is the hole or electron mobility.

Energy loss measurement

sEQE was measured using an integrated system (PECT 600, Enlitech) EQE_{EL} spectra were collected by applying external voltage (0 4 V) through the devices (ELCT 3010, Enlitech). The devices used for external quantum efficiency of electroluminescence (EQE_{EL}) was fabricated according to the optimized conditions.

$$q\Delta V = E_{gap} - qV_{oc}$$

$$= \left(E_{gap} - qV_{oc}^{SQ}\right) + \left(qV_{oc}^{SQ} - qV_{oc}^{rad}\right) + \left(qV_{oc}^{rad} - qV_{oc}\right)$$

$$= \left(E_{gap} - qV_{oc}^{SQ}\right) + q\Delta V_{oc}^{rad,\ below\ gap} + q\Delta V_{oc}^{non\ -\ rad}$$

$$= \Delta E_1 + \Delta E_2 + \Delta E_3$$

Where V_{OC}^{SQ} is the maximum voltage according to the Shockley-Queisser limit, V_{OC}^{rad} is the open-circuit voltage when there is only radiative recombination.

$$eV_{oc}^{SQ} = kT\ln\left(\frac{J_{SC,SQ}}{J_{0,SQ}} + 1\right) = kT\ln\left(\frac{e\int_{E_g}^{\infty} \emptyset_{AM1.5}(E)dE}{e\int_{E_g}^{\infty} \emptyset_{bb}(E)dE} + 1\right)$$

where $\emptyset_{AM1.5}$ is the solar radiation photon flux, $\emptyset_{bb}$ is the black body radiation at 300K.

$$eV_{oc}^{rad} = kT\ln\left(\frac{J_{SC}}{J_{0,rad}} + 1\right) = kT\ln\left(\frac{q\int_{0}^{\infty} EQE\emptyset_{AM1.5}(E)dE}{q\int_{0}^{\infty} EQE\emptyset_{bb}(E)dE} + 1\right)$$

$$q\Delta V_{oc}^{non\ -\ rad} = -kT\ln(EQE_{EL})$$

EQE_{EL} is the electroluminescence quantum efficiency of an OPV cell. In the Shockley-Queisser theory, the general quantum efficiency EQE can be defined as: the EQE is 100% above the E_g and 0 below the E_g.

TPC and TPV measurement

Transient photovoltage (TPV) and transient photocurrent (TPC) measurements were carried out under a 337 nm 3.5 ns pulse laser (160 μJ per pulse at 10 Hz) and halide lamps (150 W). Voltage and current dynamics were recorded on a digital oscilloscope (Tektronix MDO3102)

AFM and TEM characterization

Atomic force microscopy (AFM) measurements were performed on a Dimension 3100 (Veeco) Atomic Force Microscope in the tapping mode. Transmission electron microscopy (TEM) was performed using a Tecnai G2 F20 S-TWIN instrument at 200 kV accelerating voltage, in which the blend films were prepared as following: first, the blend films were spin-coated on the PEDOT:PSS/ITO substrates; second, the resulting blend film/PEDOT:PSS/ITO substrates were submerged in deionized water to make these blend films float onto the air-water interface; finally, the floated blend films were taken up on unsupported 200 mesh copper grids for a TEM measurement.

GIWAXS measurements

Grazing-incidence wide-angle X-ray scattering (GIWAXS) measurements were carried out with a Xeuss 2.0 SAXS/WAXS laboratory beamline using a Cu X-ray source (8.05k eV, 1.54 Å) and a Pilatus3R 300K detector. The incidence angle is 0.2°.

Contact Angle measurement

The contact angle tests were performed on a Dataphysics OCA40 Micro surface contact angle analyzer. The surface energy of the polymers was characterized and calculated by the contact angles of the two probe liquids (ultrapure water and diiodomethane) with the Owens and Wendt equation: $\gamma_L(1 + \cos\theta) = 2(\gamma_S^d\gamma_L^d)^{1/2} + 2(\gamma_S^p\gamma_L^p)^{1/2}$, where θ is the contact angle of a specific solvent, γ_L is the surface energy of the solvent, γ_S^d and γ_S^p refer to the dispersive and polar surface energy of the solid, respectively, and γ_L^d and γ_L^prefer to the dispersive and polar surface energy of the solvent, respectively.

Thus, the unknown value γ_S^d and γ_S^p can be solved though combining two equations obtained by contact angle measurement of two different solvents.

To calculate the wetting coefficient (ω), we should know the interfacial surface energy between different components first, which can be calculated by Neumann's equation as follows:

$$\gamma_{x-y} = \gamma_x + \gamma_y - 2\sqrt{\gamma_x \cdot \gamma_y} \cdot e^{-\beta(\gamma_x - \gamma_y)^2}$$

where $\beta = 0.000115\ m^4\ mJ^{-2}$.

The wetting coefficient of a guest material C (ω_C) in blends of host materials A and B can be further calculated by Young's equation as follows:

$$\omega_C = \frac{\gamma_{C-B} - \gamma_{C-A}}{\gamma_{A-B}}$$

The location of the material C is estimated through ω_C. If $\omega_C < -1$, material C will locate in domain B. If $-1 < \omega_C < -1$, material C will locate at the interface between material A and B. If $\omega_C > 1$, material C will locate in domain A.

Materials synthesis

Materials: All chemicals and solvents were reagent grades and purchased from Alfa

Aesar and TCI.

Compound 1 was synthesized according previous report[1], Compound 2 and compound 4 were purchased from commercial sources. Toluene and trichloromethane were freshly distilled prior to use. Compound 3 and BTR-SCl (scheme S1) were synthesized as follows:

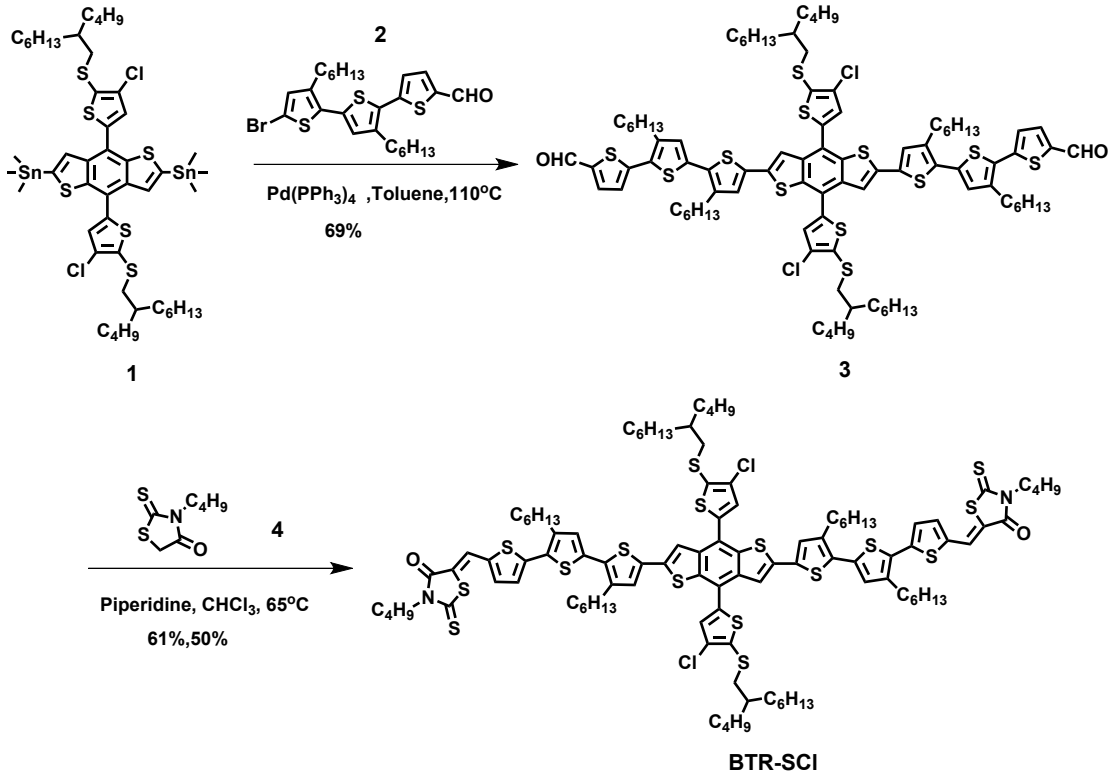

Scheme S1 Synthetic routes of BTR-SCl.

Compound 3 and BTR-SCl were synthesized as follows:

Synthesis of compound 3

In a 100 mL dried flask, compound **1** (0.98 g, 0.69 mmol), compound **2** (0.8 g, 0.153 mmol) and $Pd(PPh_3)_4$ (0.064 g, 0.08 mmol) were dissolved in anhydrous degassed toluene (50 mL). The mixture was slowly heated up to 110℃ and stirred at the temperature for 24 h under an argon atmosphere. The mixture was poured into water and extracted with CH_2Cl_2 (100 mL) for three times. The organic layer was dried over

anhydrous $MgSO_4$ and concentrated under vacuum. The crude product was purified by column chromatography on silica gel with using petroleum/CH_2Cl_2 (1:1) as eluent to obtain compound **3** as a red solid (1.1 g, 69%).^{1}H NMR (400 MHz, $CDCl_3$) δ 9.88 (s, 2H), 7.71-7.70 (d, 2H), 7.51(s, 2H), 7.32(s, 2H), 7.23-7.22(d, 2H), 7.12 (s, 2H), 7.02 (s, 2H), 3.02-3.00 (d, 4H), 2.83-2.74(m, 8H), 1.54-1.39(m, 18H),1.34-1.27(m, 44H),0.93-8.83(m, 26H).^{13}C NMR(100 MHz,) δ (ppm): 182.54, 145.96, 142.58, 142.30, 141.25, 139.81, 138.66, 138.46, 137.26, 136.82, 135.73, 134.79, 131.48, 131.07, 129.76, 129.23, 128.85, 128.76, 125.94, 122.09, 118.11, 77.35, 77.23, 77.03, 76.71, 42.52, 37.92, 33.01, 32.67, 31.84, 31.66, 30.40, 30.26, 29.81, 29.69, 29.59, 29.31, 29.28, 28.81, 26.56, 22.97, 22.69, 22.63, 14.16, 14.11, 14.09. Matrix-Assisted Laser Desorption/Ionization Time of Flight Spectrometry (MALDI-TOF) MS: calcd. For $C_{92}H_{116}Cl_2O_2S_{12}$ m/z = 1709.56; found 1708.44;

Synthesis of BTR-SCl

Compound 3 (0.2 g, 0.12 mmol) was dissolved in dry $CHCl_3$ (20 mL), and 0.5 mL piperidine and Compound 4 (0.23 g, 2.1 mmol) were added in above solution then. The reation mixture was stirred and refluxed at 65℃ for 6 h under argon. After that, the mixture was precipitated in methanol and then extracted with $CHCl_3$ for three times, the combined organic phase was washed with water and dried over anhydrous $MgSO_4$. After removal of solvent, the crude product was purified by column chromatography on silica gel with using petroleum/$CHCl_2$ (1:1) as eluent to obtain BTR-SCl as bright green solid (0.15 g, 61%).^{1}H NMR (400 MHz, $CDCl_3$) δ 7.78(s, 2H), 7.44(s, 2H), 7.32(s, 2H), 7.31-7.30(d, 2H), 7.16-7.15(d, 2H), 7.06(s, 2H), 6.97(s, 2H), 4.10-4.06(t,

4H), 3.03-3.02(d, 4H), 2.80-2.72(m, 8H), 1.54-1.28(m, 70H), 0.98-0.84(m, 34H). ^{13}C NMR (101 MHz, $CDCl_3$) δ (ppm) 182.54, 145.96, 142.58, 142.30, 141.25, 139.81, 138.66, 138.46, 137.26, 136.82, 135.73, 134.79, 131.48, 131.07, 129.76, 129.23, 128.85, 128.76, 125.94, 122.09, 118.11, 77.35, 77.23, 77.03, 76.71, 42.52, 37.92, 33.01, 32.67, 31.84, 31.66, 30.40, 30.26, 29.81, 29.69, 29.59, 29.31, 29.28, 28.81, 26.56, 22.97, 22.69, 22.63, 14.16, 14.11, 14.09. Matrix-Assisted Laser Desorption/Ionization Time of Flight Spectrometry (MALDI-TOF) MS: calcd. For $C_{104}H_{134}C_{l2}N_2O_2S_{16}$ m/z = 2052.16; found 2050.46;

Device fabrication and characterization

The non-fullerene SM-OSCs devices with a device structure of glass indium tin oxide (ITO)/poly(3,4-ethylenedioxythiophene):poly(styrenesulfonate) (PEDOT:PSS) /active layer/PFN-Br/Ag were fabricated under conditions as follows: patterned ITO-coated glass with a sheet resistance of 10-15 ohm/square was cleaned by a surfactant scrub and then underwent a wet-cleaning process inside an ultrasonic bath, beginning with deionized water followed by acetone and isopropanol. After UVO cleaning for 20 min, then a 30 nm thick PEDOT:PSS (Bayer Baytron 4083) anode buffer layer was spin-cast onto the ITO substrate and then annealed at 150 ^oC for 15 min. The optimized overall concentration was 17 mg mL^{-1} chloromethane solution with 1.4:1 (*w*/*w*) for BTR-SCl:Y6 and 1.4:1:0.1 (*w*/*w*) for BTR-SCl:Y6:PM7 respectively. Then, the blend thin film annealed with 120 °C for 10 min to improve the intermixing of the electron donor and acceptor phases. The active layer thicknesses were ~100 nm and controlled by adjusting the spinning speed during the spin-coating process and measured by an

Ambios Technology XP-2 stylus Profiler. And then a 5 nm thick PFN-Br as cathode interlayer was spin-coated on the active layer at 2500 rpm for 40 s. Finally, 150 nm Ag were successively deposited on the photosensitive layer under vacuum at a pressure of ca. 4×10^{-4} Pa. The effective area of one cell is 0.04 cm^2.

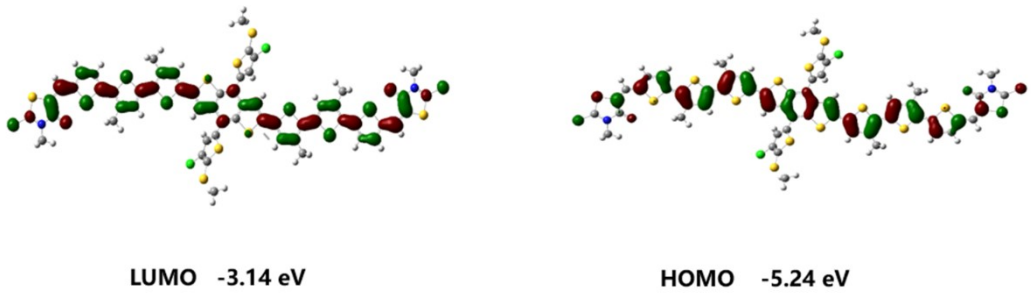

Fig. S1 Molecular energy levels and wavefunction distributions of the frontier molecular orbital for BTR-SCl by DFT.

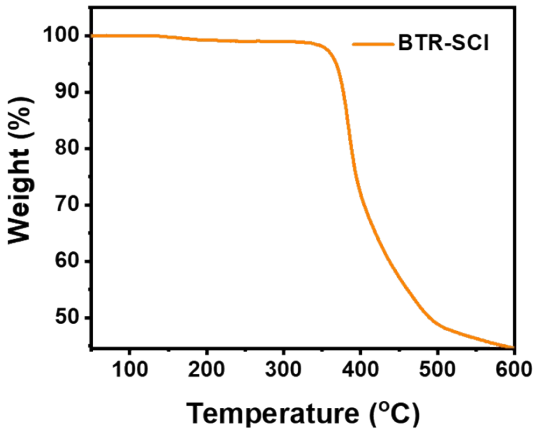

Fig. S2 The TGA curve of BTR-SCl at a scan rate of 10 °C min^{-1} under nitrogen.

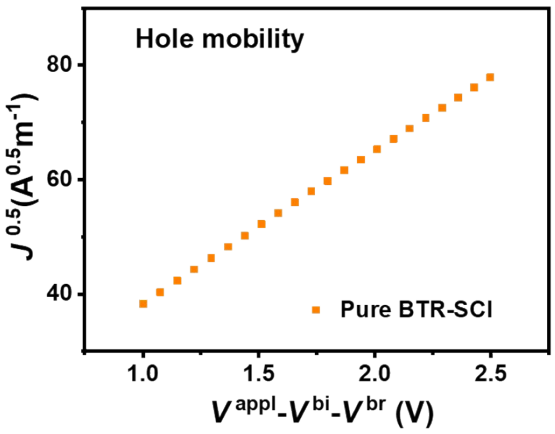

Fig. S3 The $J^{1/2}$-V plot of hole-only devices based on BTR-SCl neat film.

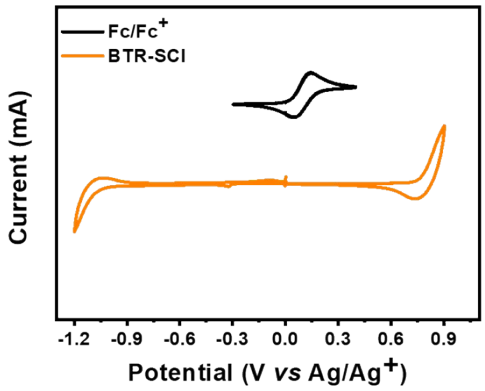

Fig. S4 Cyclic voltammogram of BTR-SCl.

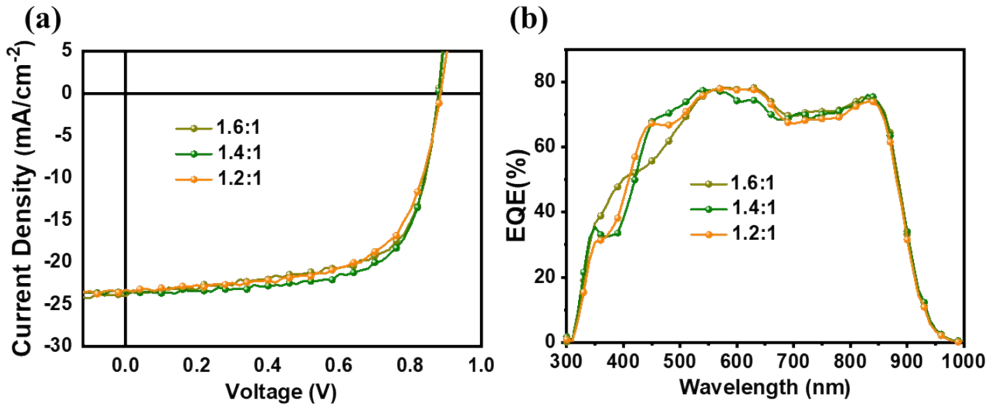

Fig. S5 (a) The *J*-*V* plots and (b) the corresponding EQE curves of the BTR-SCl:Y6 OSCs with different D/A weight ratios (TA at 120 °C for 10 min) under the illumination of AM 1.5G, 100 mW cm^{-2}.

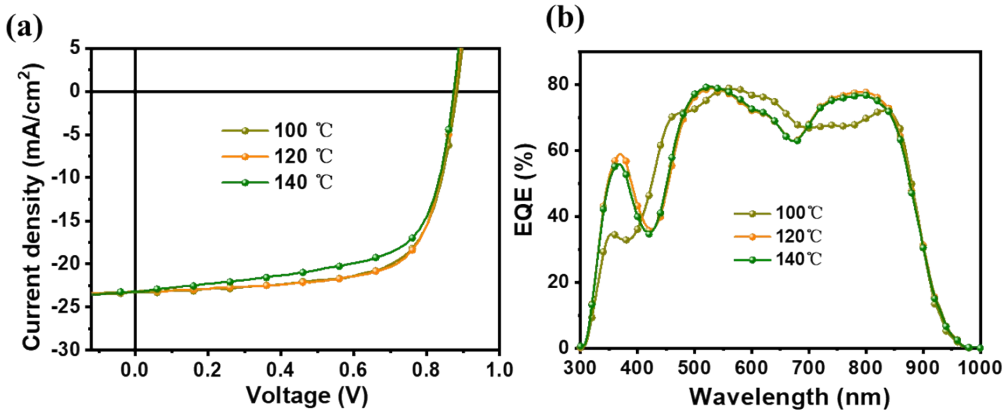

Fig. S6 (a) The *J-V* plots and (b) the corresponding EQE curves of the BTR-SCl:Y6 (1.4:1, *w/w*) with different TA temperatures for 10 min under the illumination of AM 1.5G, 100 mW cm^{-2}.

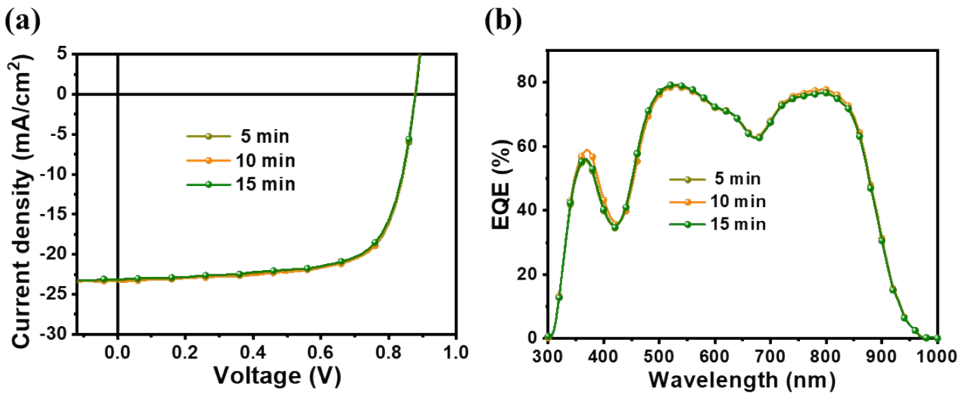

Fig. S7 (a) The *J-V* plots and (b) the EQE curves of BTR-SCl:Y6 (1.4:1, *w/w*) TA at 120 ℃ for different time under the illumination of AM 1.5G, 100 mW cm^{-2}.

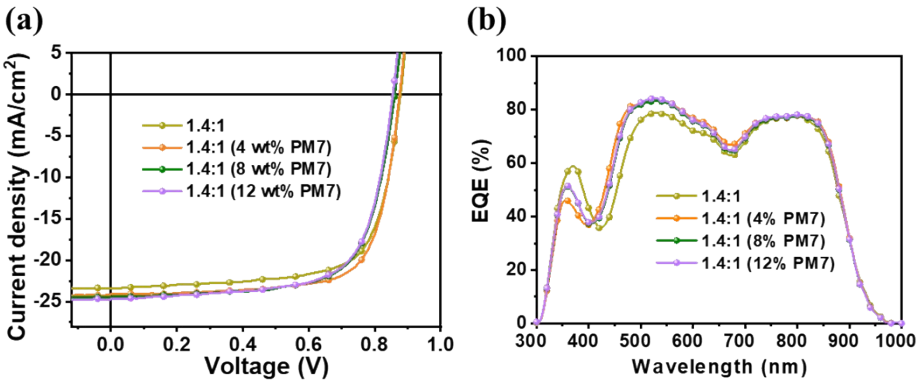

Fig. S8 (a) The *J-V* plots and (b) the corresponding EQE curves of the BTR-SCl:Y6 blend with different content PM7 (TA at 120 ℃ for 10 min) under illumination of AM 1.5G, 100 mW cm^{-2}.

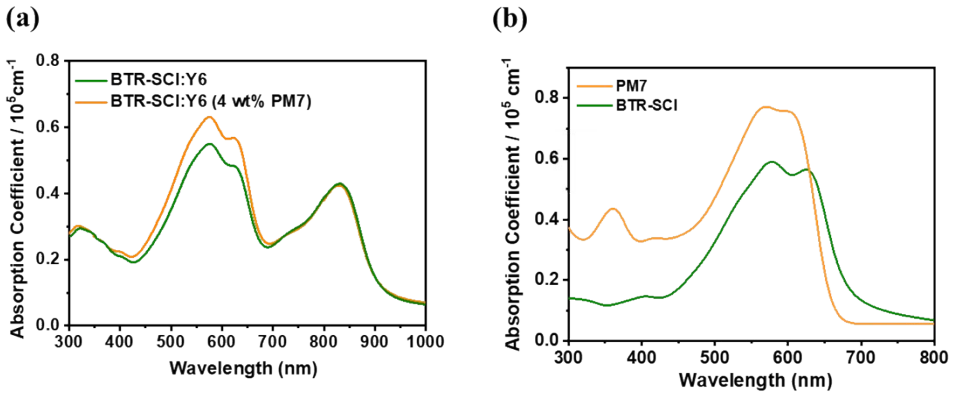

Fig. S9 The absorption coefficients of (a) BTR-SCl:Y6 blends with or without PM7 and (b) BTR-SCl and PM7 neat films.

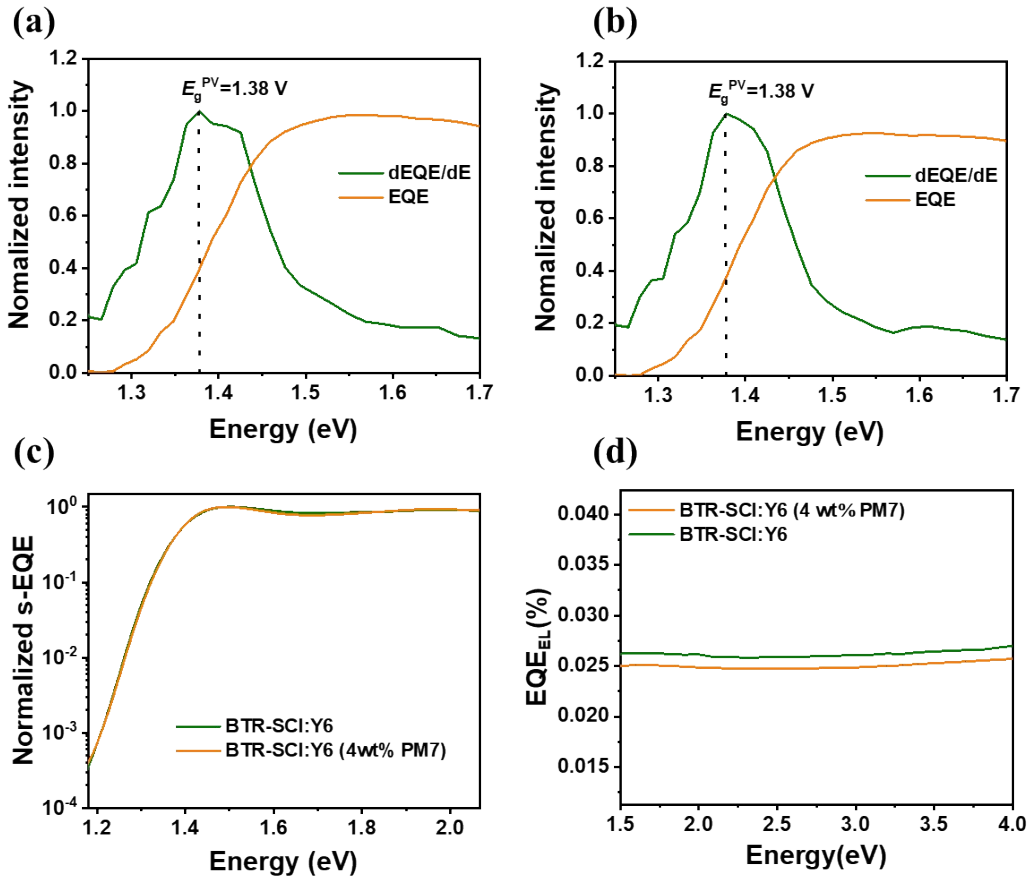

Fig. S10 (a-b) Deduction of photovoltaic bandgap from the definition of E_g^{PV} with or without PM7. (c) sEQEs spectra and (d) EQE_{EL} curve of the BTR-SCl:Y6-based device with or without PM7.

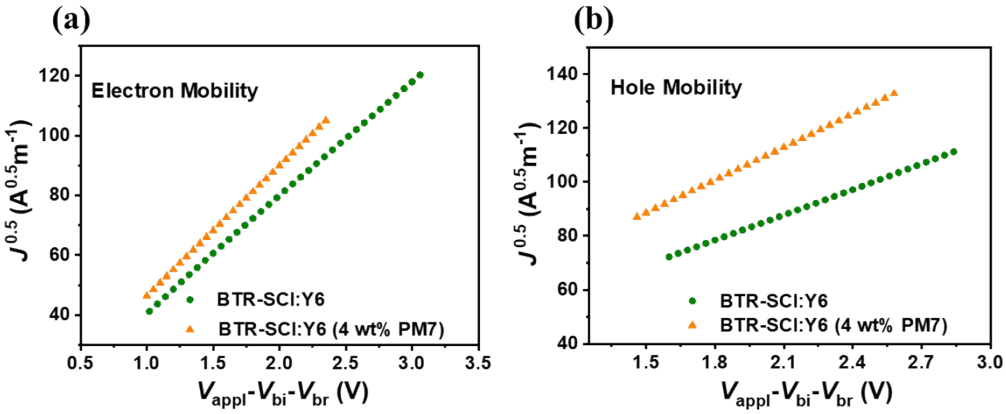

Fig. S11 The $J^{1/2}$-V curves of (a) the electron-only devices (b) the hole-only devices according to the SCLC model.

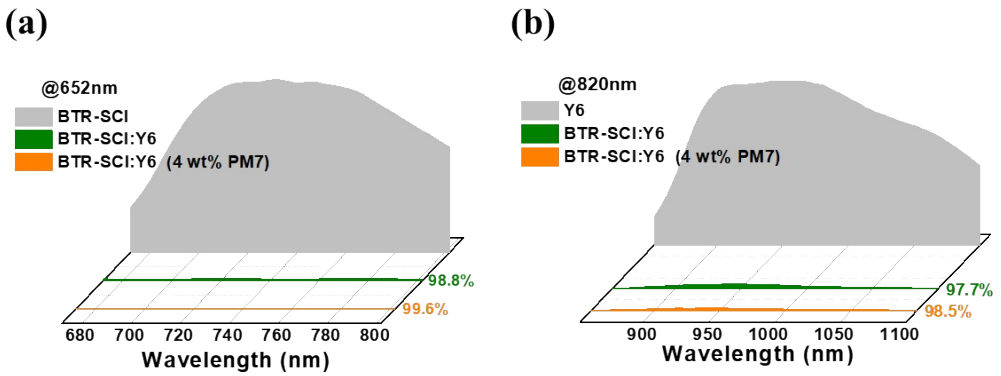

Fig. S12 The PL spectra of the (a) BTR-SCl pure film and related BTR-SCl:Y6 blends with or without PM7. (b) Y6 pure film and related BTR-SCl:Y6 blends with or without PM7.

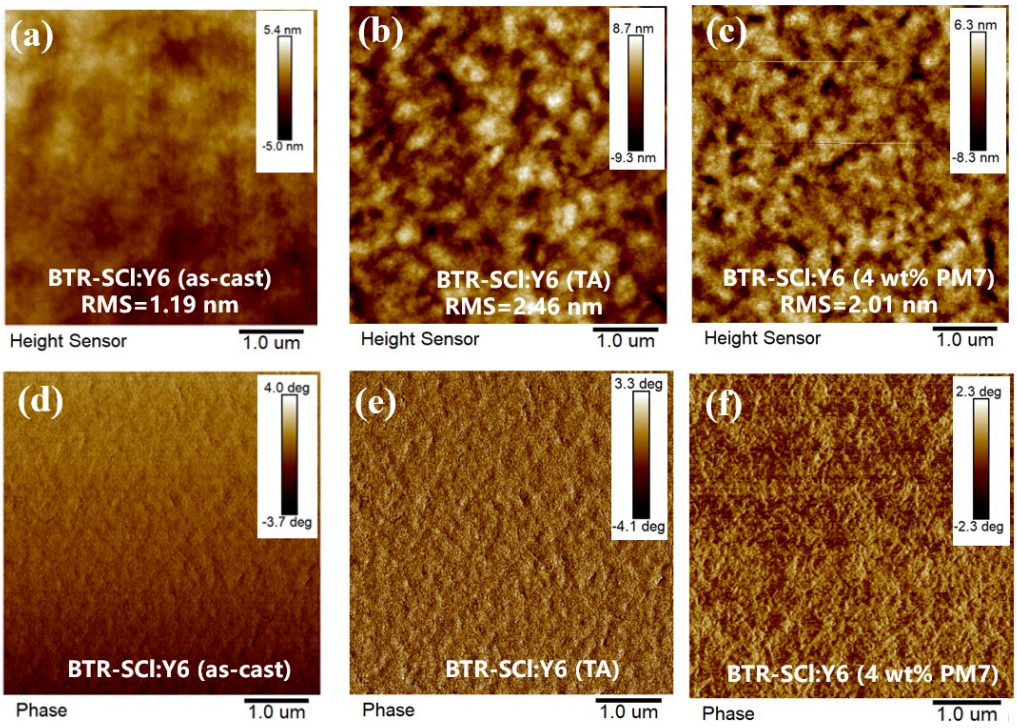

Fig. 13 The AFM height (a-c) and phase images (d-f) of the BTR-SCl:Y6 blend films under as-cast, TA, and 4 wt% PM7 condition.

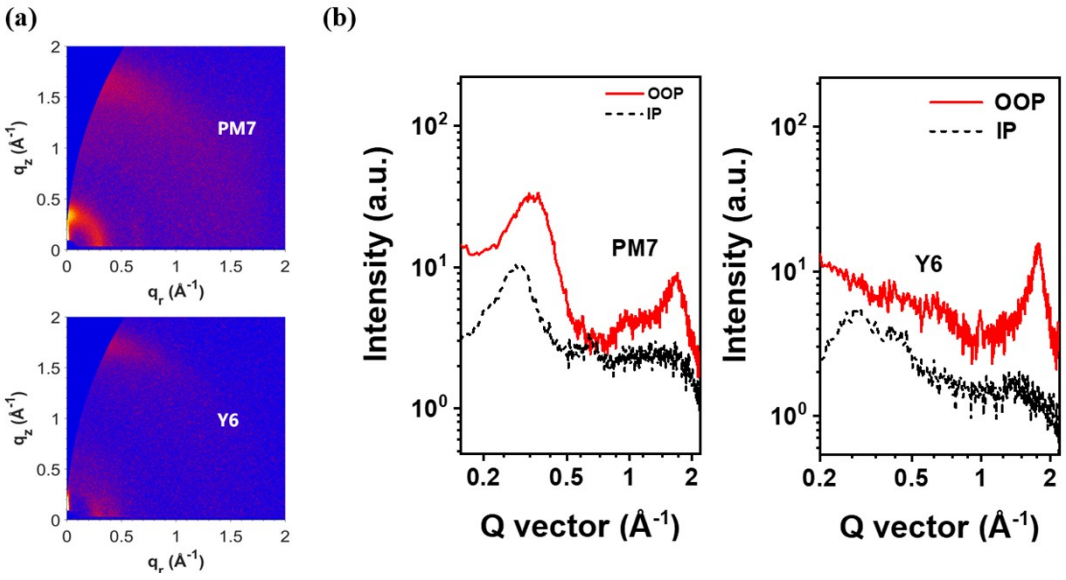

Fig. 14 (a) 2D GIWAXS profiles and (b) 1D profiles along the IP and OOP directions of PM7 and Y6 neat films.

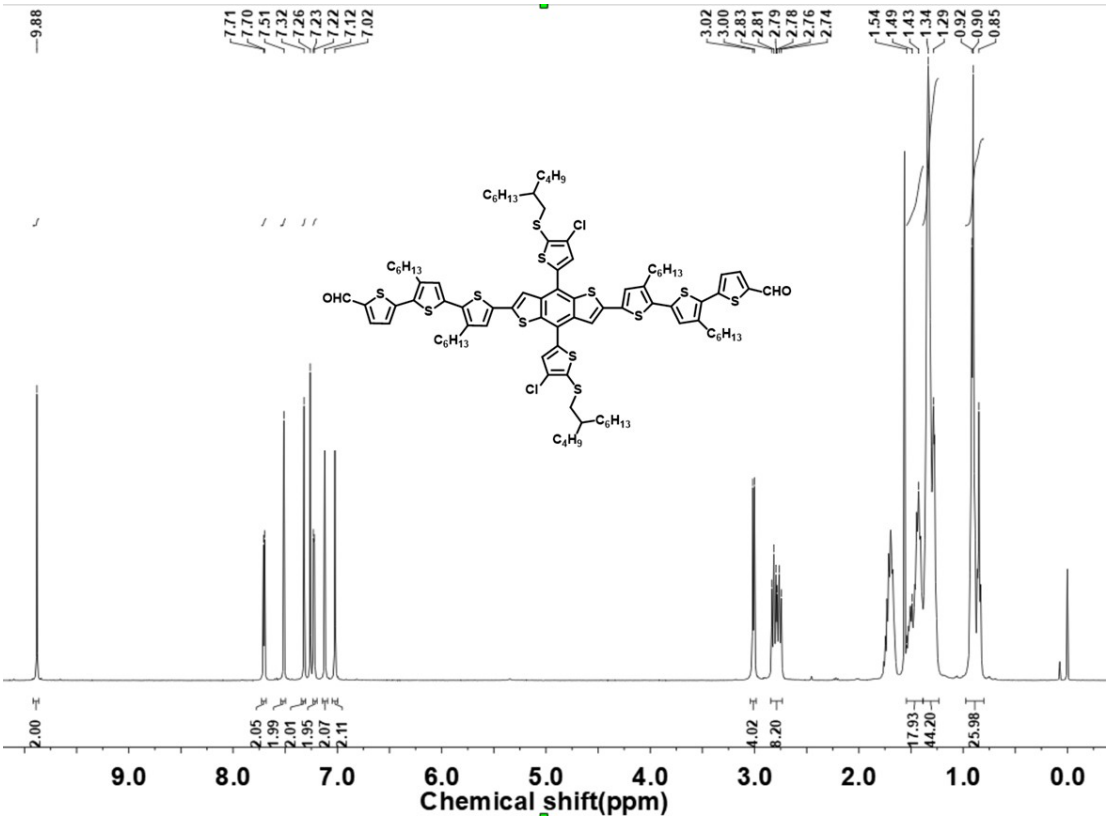

Fig. S15 ^{1}H NMR spectra of compound 3 in $CDCl_3$.

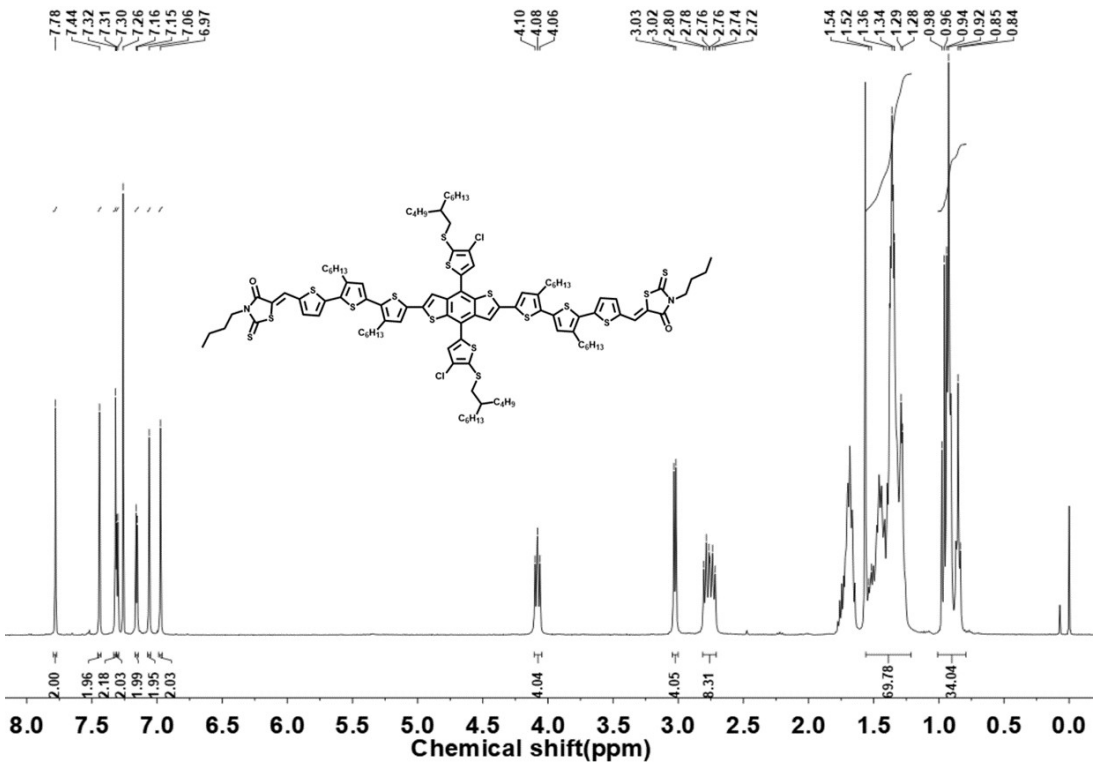

Fig. S16 ^{1}H NMR spectra of BTR-SCl in $CDCl_3$.

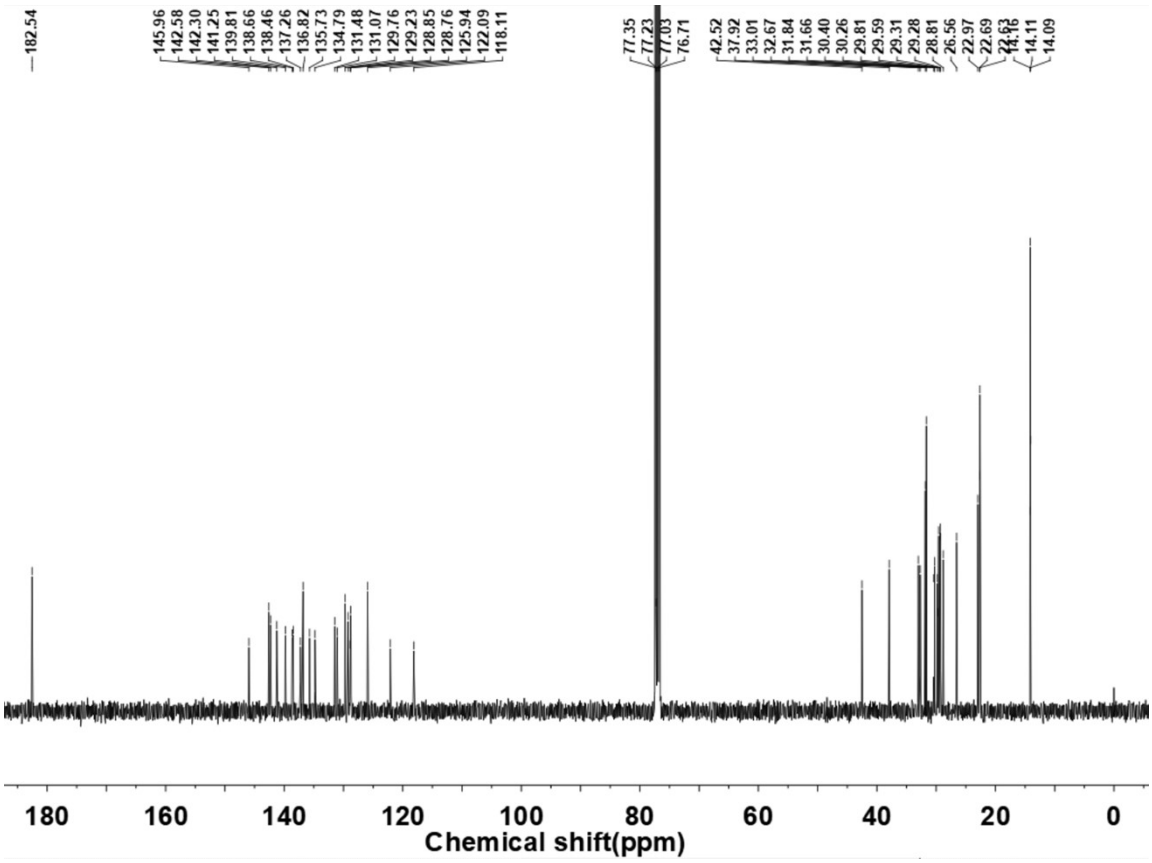

Fig. S17 ^{13}C NMR spectra of compound 3 in $CDCl_3$.

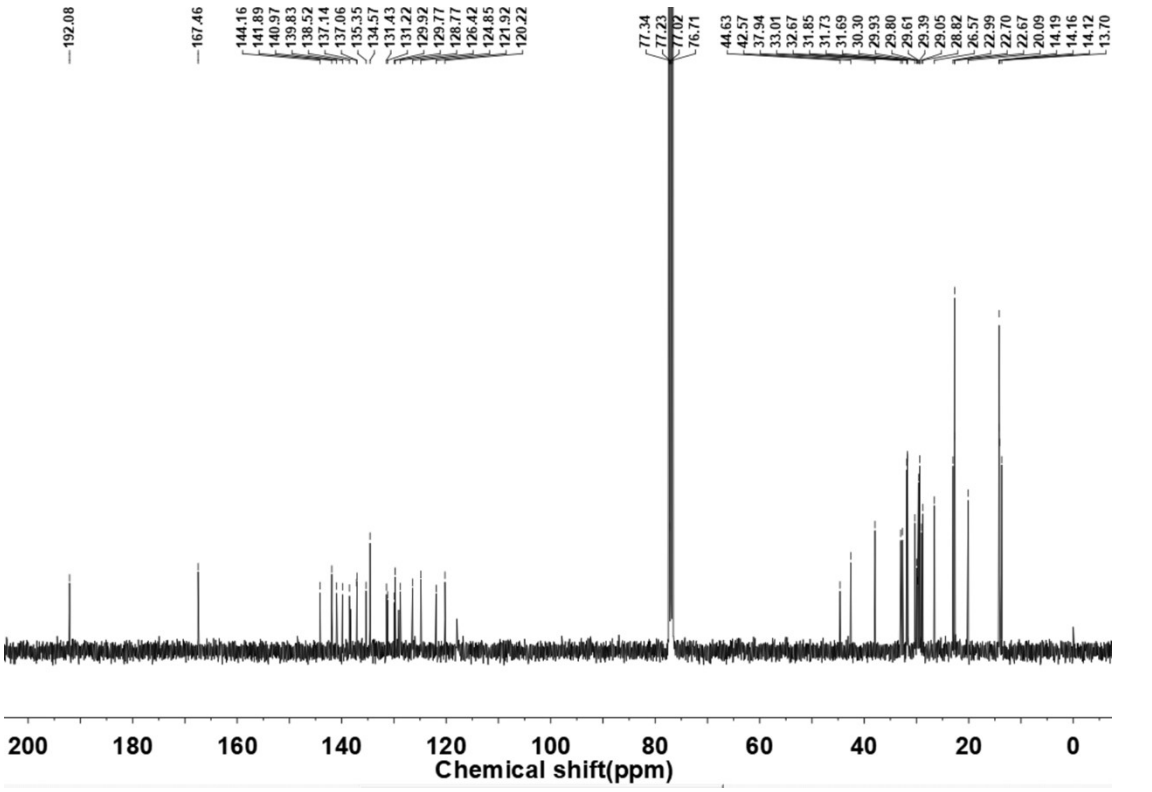

Fig. S18 ^{13}C NMR spectra of BTR-SCl in $CDCl_3$.

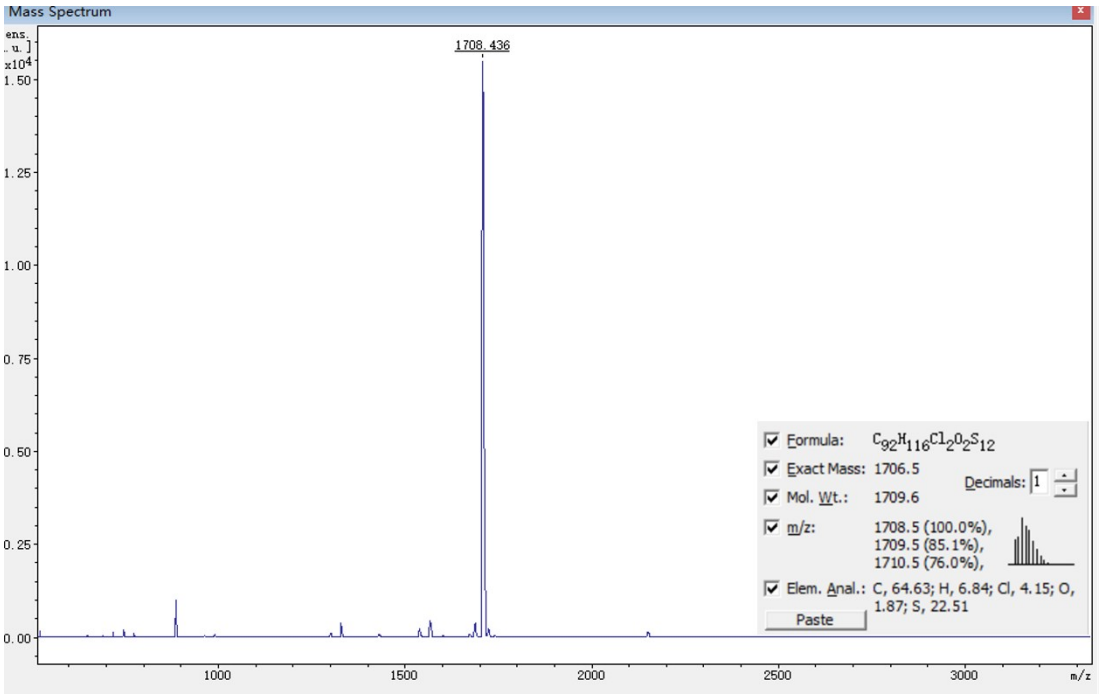

Fig. S19 MALDI-TOF spectra of compound 3.

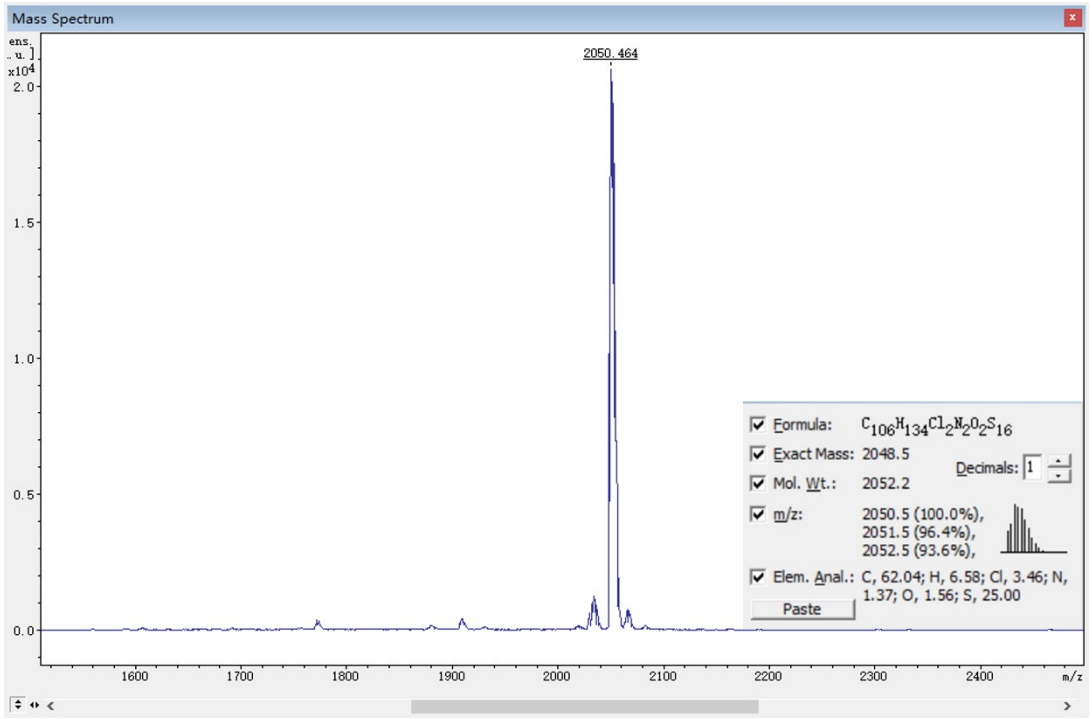

Figure S20 MALDI-TOF spectra of BTR-SCl.

Table S1 Photovoltaic data of BTR-SCl:Y6 OSCs with different D/A weight ratios (TA at 120 ℃ for 10 min) under the illumination of AM 1.5G, 100 mW cm^{-2}.

BTR-SCl:Y6	V_{oc} (V)	J_{sc} (mA cm^{-2})	Cal. J_{sc}[a]	FF (%)	PCE (%)
1.2:1	0.88	23.8	23.5	65.4	13.7
1.4:1	0.88	23.6	23.4	68.5	14.2
1.6:1	0.88	23.5	23.3	63.6	13.2

[a] The integrated J_{sc} in parenthesis from the EQE curves.

Table S2 Photovoltaic data of the OSCs based on BTR-SCl:Y6 (1.4:1, *w*/*w*) with different TA temperature for 10 min under the illumination of AM 1.5G, 100 mW cm^{-2}.

Temperature	V_{oc} (V)	J_{sc} (mA cm^{-2})	Cal. J_{sc}[a]	FF (%)	PCE (%)
As-cast	0.12	1.4	-	25.5	0.05
100 ℃	0.88	23.3	23.1	68.5	14.1
120 ℃	0.88	23.2	23.1	70.5	14.4
140 ℃	0.87	23.2	23.0	64.9	13.1

[a] The integrated J_{sc} in parenthesis from the EQE curves.

Table S3 Photovoltaic data of the OSCs based on BTR-SCl:Y6 (1.4:1, *w*/*w*) under 120 ℃ with different TA time under the illumination of AM 1.5G, 100 mW cm^{-2}.

TA time	V_{oc} (V)	J_{sc} (mA cm^{-2})	Cal. J_{sc}[a]	FF (%)	PCE (%)
5 min	0.88	23.2	23.0	71.2	14.5
10 min	0.88	23.4	23.1	70.8	14.6
15 min	0.88	23.1	23.0	70.5	14.3

[a] The integrated J_{sc} in parenthesis from the EQE curves.

Table S4 Photovoltaic parameters of OSCs based on BTR-SCl:Y6 blend with different PM7 content (TA at 120 ℃ for 10 min) under the illumination of AM 1.5G, 100 mW cm $^{-2}$.

PM7 content (wt%)	V_{oc} (V)	J_{sc} (mA cm^{-2})	Cal. J_{sc}[a]	FF (%)	PCE (%)
0	0.88	23.4	23.1	70.8	14.6
4	0.88	24.5	24.1	73.1	15.8
8	0.86	24.5	24.2	69.8	14.7
12	0.85	24.7	24.3	69.0	14.5

[a] The integrated J_{sc} in parenthesis from the EQE curves.

Table S5. Summary of recent photovoltaic parameters for high-performance NFA ASM-OSCs devices (PCE>9%).

Active Layer	V_{oc} (V)	PCE (%)	Ref.
DRTB-T:IC-C6IDT-IC	0.98	9.08	[2]
DRTB-T:IDIC	0.98	9.06	[3]
H11:IDIC	0.98	9.73	[4]
SM1:IDIC	0.91	10.11	[5]
H22:IDIC	0.94	10.29	[6]
DRTB-T-C4:IT-4F	0.91	11.24	[7]
BDT3TR-SF:NBDTP-Fout	0.80	11.25	[8]
ZnP-TBO:6TIC	0.80	12.08	[9]
BSFTR:NBDTP-F_{out}	0.80	12.26	[10]
BTR-Cl:Y6	0.86	13.61	[11]
BSFTR:Y6	0.85	13.69	[12]
BTTzR:Y6	0.88	13.90	[13]
SM1-F:Y6	0.86	14.07	[14]

ZR1:Y6	0.86	14.34	[15]
BTR-SCl:Y6	0.88	14.6	This work
B1:BO-4Cl	0.83	15.3	[16]
BTR-Cl:Y6:$PC_{71}BM$	0.84	15.34	[17]
BT-2F:N3	0.85	15.39	[18]
ZR-TT:Y6 (3%PJ1)	0.81	15.54	[19]
SM-BF1:Y6	0.85	15.71	[20]
BTR-SCl:Y6 (4wt% PM7)	0.88	15.8	This work
L2:Y6	0.83	15.80	[21]
ZnP-TSEH: 6TIC: 4TIC	0.81	15.88	[22]
M-PhS:BTP-eC9	0.84	16.2	[23]
B1:BO-4Cl:Y7	0.84	16.28	[24]
B1:BO-2Cl:BO-4Cl	0.84	17.0	[25]

Table S6. Summary of photovoltaic parameters for recent high-performance PSCs based on SMDs as a third component.

Active Layer	V_{oc} (V)	PCE (%)	Ref.
PM6:SM1:Y6	0.831	16.55	[26]
PM6:BPR-SCl:Y6	0.87	16.74	[27]
PM6:BTBr-2F:Y6	0.859	17.38	[28]
PM6:BTTzR:Y6	0.87	17.7	[29]
PM6:BPR-SCl:BTP-eC9	0.856	18.02	[30]
D18-Cl:G19:Y6	0.87	18.53	[31]

Table S7 E_{loss} paramaters of BTR-SCl:Y6-based OSCs with or without PM7.

Active layer	V_{oc} (V)	E_g^{PV} (eV)	E_{loss} (eV)	ΔE_1 (eV)	ΔE_2 (eV)	EQE_{EL} (%)	ΔE_3 (eV)
BTR-SCl:Y6	0.88	1.38	0.50	0.26	0.03	2.6×10^{-2}	0.21
BTR-SCl:Y6 (4 wt% PM7)	0.88	1.38	0.50	0.26	0.03	2.5×10^{-2}	0.21

Table S8 GIWAXS parameters of the pure films and the corresponding blend films.

Component	Peak	Position ($Å^{-1}$)	D-spacing (Å)	FWHM ($Å^{-1}$)	Coherence length (Å)
BTR-SCl	(100) IP	0.31	20.53	0.31	18.48
	(010) IP	1.74	3.62	0.14	39.27
	(010) OOP	1.68	3.74	0.37	15.28
	(100) OOP	0.31	20.14	0.02	297.63
	(200) OOP	0.62	10.22	0.04	141.37
	(300) OOP	0.92	6.85	0.06	100.98
PM7	(100) IP	0.29	21.74	0.12	49.17
	(010) OOP	1.67	3.77	0.34	16.73
Y6	(100) IP	0.29	21.74	0.12	47.92
	(010) OOP	1.77	3.55	0.15	37.20
BTR-SCl:Y6 (as-cast)	(100) IP	0.30	21.23	0.09	66.53
	(100) OOP	0.31	20.40	0.10	55.99
BTR-SCl:Y6 (TA)	(100) IP	0.30	20.87	0.05	106.70
	(100) OOP	0.31	20.20	0.04	157.08
BTR-SCl:Y6 (4 wt%PM7)	(100) IP	0.30	20.87	0.05	113.10
	(010) OOP	1.75	3.59	0.21	27.19
	(100) OOP	0.31	20.33	0.04	128.52

References

1 S. Park, H. Ahn, J.-y. Kim, J. B. Park, J. Kim, S. H. Im and H. J. Son, *ACS Energy Lett.*, 2019, **5**, 170-179.

2 L. Yang, S. Zhang, C. He, J. Zhang, H. Yao, Y. Yang, Y. Zhang, W. Zhao and J. Hou, *J. Am. Chem. Soc*., 2017, **139**, 1958-1966.

3 S. Zhang, L. Yang, D. Liu, C. He, J. Zhang, Y. Zhang and J. Hou, *Sci. China Chem.*, 2017, **60**, 1340-1348.

4 H. Bin, Y. Yang, Z. G. Zhang, L. Ye, M. Ghasemi, S. Chen, Y. Zhang, C. Zhang, C. Sun, L. Xue, C. Yang, H. Ade and Y. Li, *J. Am. Chem. Soc.*, 2017, **139**, 5085-5094.

5 B. Qiu, L. Xue, Y. Yang, H. Bin, Y. Zhang, C. Zhang, M. Xiao, K. Park, W. Morrison, Z.-G. Zhang and Y. Li, *Chem. Mater.*, 2017, **29**, 7543-7553.

6 H. Bin, J. Yao, Y. Yang, I. Angunawela, C. Sun, L. Gao, L. Ye, B. Qiu, L. Xue, C. Zhu, C. Yang, Z. G. Zhang, H. Ade and Y. Li, *Adv. Mater.*, 2018, **30**, 1706361.

7 L. Yang, S. Zhang, C. He, J. Zhang, Y. Yang, J. Zhu, Y. Cui, W. Zhao, H. Zhang, Y. Zhang, Z. Wei and J. Hou, *Chem. Mater.*, 2018, **30**, 2129-2134.

8 H. Wu, H. Fan, S. Xu, L. Ye, Y. Guo, Y. Yi, H. Ade and X. Zhu, *Small*, 2019, **15**, 1804271.

9 K. Gao, S. B. Jo, X. Shi, L. Nian, M. Zhang, Y. Kan, F. Lin, B. Kan, B. Xu, Q. Rong, L. Shui, F. Liu, X. Peng, G. Zhou, Y. Cao and A. K. Jen, *Adv. Mater.*, 2019, **31**,

1807842.

10 H. Wu, Q. Yue, Z. Zhou, S. Chen, D. Zhang, S. Xu, H. Zhou, C. Yang, H. Fan and X. Zhu, *J. Mater. Chem. A*, 2019, **7**, 15944-15950.

11 H. Y. Chen, D. Q. Hu, Q. G. Yang, J. Gao, J. H. Fu, K. Yang, H. He, S. S. Chen, Z. P. Kan, T. N. Duan, C. Yang, J. Y. Ouyang, Z. Y. Xiao, K. Sun and S. R. Lu, *Joule*, 2019, **3**, 3034-3047.

12 Q. Yue, H. Wu, Z. Zhou, M. Zhang, F. Liu and X. Zhu, *Adv. Mater.*, 2019, **31**, 1904283.

13 Y. Wang, Y. Wang, L. Zhu, H. Liu, J. Fang, X. Guo, F. Liu, Z. Tang, M. Zhang and Y. Li, *Energy Environ. Sci.*, 2020, **13**, 1309-1317.

14 B. Qiu, Z. Chen, S. Qin, J. Yao, W. Huang, L. Meng, H. Zhu, Y. M. Yang, Z. G. Zhang and Y. Li, *Adv. Mater.*, 2020, **32**, 1908373.

15 R. Zhou, Z. Jiang, C. Yang, J. Yu, J. Feng, M. A. Adil, D. Deng, W. Zou, J. Zhang, K. Lu, W. Ma, F. Gao and Z. Wei, *Nat. Commun.*, 2019, **10**, 5393.

16 J. Qin, C. An, J. Zhang, K. Ma, Y. Yang, T. Zhang, S. Li, K. Xian, Y. Cui, Y. Tang, W. Ma, H. Yao, S. Zhang, B. Xu, C. He and J. Hou, *Sci. China Mater.*, 2020, **63**, 1142-1150.

17 D. Hu, Q. Yang, H. Chen, F. Wobben, V. M. Le Corre, R. Singh, T. Liu, R. Ma, H. Tang, L. J. A. Koster, T. Duan, H. Yan, Z. Kan, Z. Xiao and S. Lu, *Energy Environ. Sci.*, 2020, **13**, 2134-2141.

18 J. Ge, L. Hong, W. Song, L. Xie, J. Zhang, Z. Chen, K. Yu, R. Peng, X. Zhang and Z. Ge, *Adv. Energy Mater.*, 2021, **11**, 2100800.

19 Z. Zhang, D. Deng, Y. Li, J. Ding, Q. Wu, L. Zhang, G. Zhang, M. J. Iqbal, R. Wang, J. Zhang, X. Qiu and Z. Wei, *Adv. Energy Mater.*, 2021, **12**, 2102394.

20 J. Guo, B. Qiu, D. Yang, C. Zhu, L. Zhou, C. Su, U. S. Jeng, X. Xia, X. Lu, L. Meng, Z. Zhang and Y. Li, *Adv. Funct. Mater.*, 2021, **32**, 2110159.

21 T. Xu, J. Lv, K. Yang, Y. He, Q. Yang, H. Chen, Q. Chen, Z. Liao, Z. Kan, T. Duan, K. Sun, J. Ouyang and S. Lu, *Energy Environ. Sci.*, 2021, **14**, 5366-5376.

22 L. Nian, Y. Kan, K. Gao, M. Zhang, N. Li, G. Zhou, S. B. Jo, X. Shi, F. Lin, Q. Rong, F. Liu, G. Zhou and A. K. Y. Jen, *Joule*, 2020, **4**, 2223-2236.

23 L. Zhang, X. Zhu, D. Deng, Z. Wang, Z. Zhang, Y. Li, J. Zhang, K. Lv, L. Liu, X. Zhang, H. Zhou, H. Ade and Z. Wei, *Adv. Mater.*, 2021, **34**, 2106316.

24 M. Jiang, H. Bai, H. Zhi, L. Yan, H. Y. Woo, L. Tong, J. Wang, F. Zhang and Q. An, *Energy Environ. Sci.*, 2021, **14**, 3945-3953.

25 J. Qin, Z. Chen, P. Bi, Y. Yang, J. Zhang, Z. Huang, Z. Wei, C. An, H. Yao, X. Hao, T. Zhang, Y. Cui, L. Hong, C. Liu, Y. Zu, C. He and J. Hou, *Energy Environ. Sci.*, 2021, **14**, 5903-5910.

26 T. Yan, J. Ge, T. Lei, W. Zhang, W. Song, B. Fanady, D. Zhang, S. Chen, R. Peng and Z. Ge, *J. Mater. Chem. A*, 2019, **7**, 25894.

27 X. Chen, Q. Zhang, D. Wang, X. Xu, Z. Wang, Y. Li, H. Zhu, X. Lu, W. Chen, H. Qiu and C.-Z. Li, *Solar RRL*, 2020, **4**, 2000537.

28 L. Xu, W. Tao, H. Liu, J. Ning, M. Huang, B. Zhao, X. Lu and S. Tan, *J. Mater. Chem. A*, 2021, **9**, 11734.

29 Q. Liu, Y. Wang, J. Fang, H. Liu, L. Zhu, X. Guo, M. Gao, Z. Tang, L. Ye, F. Liu,

M. Zhang and Y. Li, *Nano Energy*, 2021, **85**, 105963.

30 X. Chen, D. Wang, Z. Wang, Y. Li, H. Zhu, X. Lu, W. Chen, H. Qiu and Q. Zhang, *Chem. Eng. J.*, 2021, **424**, 130397.

31 Z. Chen, W. Song, K. Yu, J. Ge, J. Zhang, L. Xie, R. Peng and Z. Ge, *Joule*, 2021, **5**, 2395.